

Electromagnetic outflows in scalar-tensor theories vs General Relativity: binary neutron star coalescence

Marcelo Ponce,¹ Carlos Palenzuela,^{2,3} Enrico Barausse,^{4,5} and Luis Lehner^{6,7}

¹*Department of Physics, University of Guelph, Guelph, Ontario N1G 2W1, Canada.*

²*Canadian Institute for Theoretical Astrophysics, Toronto, Ontario M5S 3H8, Canada.*

³*Departament de Física, Universitat de les Illes Balears and Institut d'Estudis Espacials de Catalunya, Cra. Valldemossa Km 7.5, E-07122 Palma de Mallorca, Spain.*

⁴*CNRS, UMR 7095, Institut d'Astrophysique de Paris, 98bis Bd Arago, 75014 Paris, France.*

⁵*Sorbonne Universités, UPMC Univ Paris 06, UMR 7095, 98bis Bd Arago, 75014 Paris, France.*

⁶*Perimeter Institute for Theoretical Physics, Waterloo, Ontario N2L 2Y5, Canada.*

⁷*CIFAR, Cosmology & Gravity Program, Toronto, ON M5G 1Z8, Canada.*

(Dated: November 23, 2022)

As we showed in previous work, the dynamics and gravitational emission of binary neutron star systems in scalar-tensor theories can differ significantly from that expected from General Relativity in the coalescing stage. In this work we examine whether the characteristics of the electromagnetic counterparts to these binaries – driven by magnetosphere interactions prior to the merger event – can provide an independent way to test gravity in the most strongly dynamical stages of binary mergers. We find that the electromagnetic flux emitted by binaries in scalar-tensor theories can show deviations from the GR prediction in particular cases. These differences are quite subtle, thus requiring delicate measurements to differentiate between GR and the type of scalar-tensor theories considered in this work using electromagnetic observations alone. However, if coupled with a gravitational-wave detection, electromagnetic measurements might provide a way to increase the confidence with which GR will be confirmed (or ruled out) by gravitational observations.

PACS numbers:

I. INTRODUCTION

General Relativity (GR) has been very successful at describing gravity in a vast range of scales, from submillimeter ones [1], to those of the Earth, Solar system [2] and binary pulsars [3–7]. This beautiful theory, however, is known to be incomplete in the ultra-violet regime where it must be replaced by a quantum theory of gravity. Furthermore, at the infra-red cosmological scales, it needs to be supplemented with Dark Matter and an unnaturally valued cosmological constant to explain observations, which can also be interpreted as a sign of failure. These reasons have spurred intense, and ongoing, efforts exploring how to describe gravity at both classical and quantum levels, the latter being one of the most challenging enterprises of modern physics.

Restricting to the classical regime –where both laboratory experiments and astrophysical observations can help constrain possible alternatives– a large number of putative theories have already been significantly constrained or ruled out altogether (see e.g. Refs. [8, 9]). In the particular case of astrophysical observations, binaries involving pulsars have proved especially well suited for these studies [3–7]. Indeed, exquisite electromagnetic observations of the pulsar signal allow following the binary's orbital dynamics and comparing it with predictions from GR and other theories. To date this task has necessarily involved binaries at relatively large separations and, correspondingly, low orbital velocities ($v/c \ll 1$). Binaries in such configurations, as a consequence, do not fully explore possible discrepancies that might arise at relativis-

tic velocities $v/c \simeq 1$. Such discrepancies include dipolar emission of non-tensorial gravitational waves [10–14], as well as dynamical violations of the (strong) equivalence principle and enhancement of the strength of the gravitational attraction in the last, highly relativistic stages of the binary inspiral and plunge [15–17].

Such status of affairs will soon be radically changed thanks to a network of gravitational wave detectors that will allow analyzing compact binaries in highly relativistic velocity regimes. The detection of gravitational waves from these systems will not only allow testing GR, but will additionally provide important clues about the physical nature of these binaries, as well as identify the source's location. This knowledge may help – both directly and indirectly – identify electromagnetic counterparts (e.g. Refs. [18–21]) to these systems. The synergy of gravitational and electromagnetic observations will permit in-depth “multi-messenger” investigation of the behavior of gravity in such highly relativistic binaries. For this analysis to be possible, on the gravitational-wave side it is important that possible deviations from the predictions of GR are either understood, or suitably parameterized¹, so as to guide the detection and analysis of possible signals. Activities in both these fronts have recently been gaining significant momentum: In the “parameterized” approach particular formalisms have been presented, motivated by specific theories and phenomenological con-

¹ See discussion in e.g. Ref. [22].

siderations. Such formalisms have been applied to derive bounds on the relevant parameters describing deviations from GR [23–25]. In the “direct” approach, deviations from the gravitational waves predicted by GR are computed in specific bona-fide gravity theories (i.e. ones with a well-defined initial value problem) [15–17, 26–28], and the prospects for detecting these deviations are analyzed [22, 29]. Among these theories, scalar-tensor (ST) theories [30–35] – where gravity is mediated not only by a metric tensor but also by a scalar field – have received the most attention, because the presence of a scalar field in nature is motivated by e.g., the low-energy limit of string theories, the observation of the Higgs boson, and cosmological phenomenology (i.e. inflation and Dark Energy).

Among the most likely sources of gravitational waves for Earth-based detectors is the coalescence of binary neutron stars. The study of such systems in ST theories has been traditionally undertaken via suitable perturbation expansions [11, 12, 14, 27], and more recently via numerical simulations [15, 16] or a hybrid approach [17]. These works have not only provided definitive predictions for the expected signals but also helped illustrate that strong deviations from GR could arise due to dynamically-induced effects as the orbit tightens [15]. A first analysis indicating how such differences could be detected in the near future (by the upcoming second generation of gravitational wave interferometers) has been presented in Ref. [29]. As mentioned, among the possible physical parameters that can be obtained via gravitational wave observations are the time (and frequency) of the merger as well as the sky location, both of which would aid follow-up efforts to capture counterparts in a wide range of electromagnetic bands. Within GR, much effort has been going into identifying promising near-coalescence scenarios able to yield detectable signals in the electromagnetic spectrum, and a number of mechanisms have been proposed and explored in recent years (e.g. in Refs. [19, 36–41]). It is therefore interesting to consider whether electromagnetic signals (either on their own, or in combination with gravitational wave observations) can provide additional clues as to whether gravity behaves as predicted by GR. This is especially important as facilities for gravitational wave observations will be for years much more restricted in the frequency window they can access in comparison to the large spectra provided by diverse electromagnetic observatories. To this goal, we consider here whether electromagnetic counterparts triggered during the coalescence stage of neutron-star binaries can provide such testing opportunities. In particular we here study the electromagnetic energy flux produced as a result of magnetosphere interactions in ST and GR theories. We take advantage of the hybrid approach presented in Ref. [17] together with an enhanced unipolar model to describe the electromagnetic induced luminosity studied in Refs. [36, 37, 42] (and related to previous works [43–45]).

This paper is organized as follows: in section II we

review the ST theories considered, and we describe the procedure that we use to obtain the dynamics and estimate the electromagnetic luminosities; in section III we present the cases considered and the results obtained; and finally in section IV we discuss the implications of our work.

II. METHODS

In this work we are primarily concerned with estimating possible electromagnetic signals from the coalescence of magnetized binary neutron stars in GR and ST theories. We obtain the binary’s dynamics by solving the 2.5 PN equations of motion for ST theories as described in Ref. [27] (enhanced with the formalism proposed and validated in Ref. [17] to account for the scalarization effects allowed by the theories). The electromagnetic radiation induced by magnetospheric interactions of the magnetized neutron stars is estimated using a phenomenological model based on an extension of the unipolar inductor. Such model captures magnetospheric effects by considering the electromotive force (emf) that is induced as an otherwise non-magnetized conductor moves through a magnetic field [44, 45]. We have augmented this model recently in Ref. [36, 42] to account for an additional “shielding effect” that arises when both stars are magnetized, and which modifies the radius at which the emf induction takes place.

A. Scalar-tensor theories

1. Dynamics in ST theories and equations of motion

The action for a ST theory can be written in the Jordan frame as

$$S = \int d^4x \frac{\sqrt{-g}}{2\kappa} \left[\phi R - \frac{\omega(\phi)}{\phi} \partial_\mu \phi \partial^\mu \phi \right] + S_M[g_{\mu\nu}, \psi], \quad (1)$$

where $\kappa = 8\pi G$, R , g and ϕ are respectively the Ricci scalar, the metric determinant and the scalar field, and the theory has no potential for the scalar field, but is characterized by an arbitrary function $\omega(\phi)$ (and by the boundary conditions for the scalar field). Note also that in this action we have assumed that the matter degrees of freedom ψ couple minimally to the metric (and not to the scalar field) so as to enforce the weak equivalence principle (i.e. the universality of free fall for weakly gravitating bodies). The Jordan frame action can be recast in a more convenient form by a conformal transformation to the “Einstein frame”, i.e. by defining a new metric $g_{\mu\nu}^E$ and a new scalar φ such that $g_{\mu\nu}^E = \phi g_{\mu\nu}$ and $(d \log \phi / d\varphi)^2 = 2\kappa / [3 + 2\omega(\phi)]$. This transforma-

tion casts the action (1) in the form

$$S = \int d^4x \sqrt{-g^E} \left(\frac{R^E}{2\kappa} - \frac{1}{2} g_{\mu\nu}^E \partial_\mu \varphi \partial_\nu \varphi \right) + S_M \left[\frac{g_{\mu\nu}^E}{\phi(\varphi)}, \psi \right] \quad (2)$$

where note that the matter degrees of freedom still couple only to the Jordan frame metric $g_{\mu\nu} = g_{\mu\nu}^E/\phi$ (i.e. test particles follow geodesics of $g_{\mu\nu}$ and *not* ones of $g_{\mu\nu}^E$), and that $g_{\mu\nu}^E$ and φ are coupled minimally in the absence of matter (which explains why using Einstein frame variables is advantageous).

By varying the Einstein frame action, one obtains the field equations

$$G_{\mu\nu}^E = \kappa (T_{\mu\nu}^\varphi + T_{\mu\nu}^E), \quad (3)$$

$$\square^E \varphi = \frac{1}{2} \frac{d \log \phi}{d\varphi} T_E, \quad (4)$$

$$\nabla_\mu^E T_E^{\mu\nu} = -\frac{1}{2} T_E \frac{d \log \phi}{d\varphi} g_{\mu\nu}^E \partial_\mu \varphi, \quad (5)$$

where we assume that indices are raised and lowered with $g_{\mu\nu}^E$ and define $T_E \equiv T_E^{\mu\nu} g_{\mu\nu}^E$. Note that we also define the stress energy tensors appearing in the field equations as

$$T_E^{\mu\nu} = \frac{2}{\sqrt{-g^E}} \frac{\delta S_M}{\delta g_{\mu\nu}^E} = T^{\mu\nu} \phi^{-3} \quad (6)$$

$$T_{\mu\nu}^\varphi = \partial_\mu \varphi \partial_\nu \varphi - \frac{g_{\mu\nu}^E}{2} g_E^{\alpha\beta} \partial_\alpha \varphi \partial_\beta \varphi \quad (7)$$

where $T^{\mu\nu}$ is the Jordan frame stress-energy tensor of all the matter degrees of freedom.

Solutions to Eqs. (3)–(5) for binary systems of compact objects (e.g. neutron stars or black holes) can be obtained numerically in the late stages of the inspiral and during the merger [15, 16, 46], but in order to describe more widely separated systems such as observed binary pulsars, it is more convenient to expand the field equations in Post-Newtonian orders. In such a scheme, one approximates the two objects as point particles with masses m_i and sensitivity parameters s_i [10] (or equivalently scalar charges [12] $\alpha_i = -(2s_i - 1)/(3 + 2\omega_0)^{1/2}$, with ω_0 the value of the function $\omega(\phi)$ far from the binary system). The sensitivities can be calculated from isolated solutions for the compact objects, and depend on the ST theory and on the object’s compactness (e.g. $s_i \approx 0$ for white dwarfs and less compact stars, $s_i = 1/2$ for black holes, while for neutron stars the sensitivity depends critically on the star’s compactness and the ST theory under consideration). The binary’s dynamics is then expanded in orders of v/c (v being the binary’s relative velocity), and to 2.5 PN order the resulting equations

take the schematic form [11, 12, 14, 27]

$$\begin{aligned} \frac{d^2 \mathbf{x}}{dt^2} = & -\frac{G_{\text{eff}} M}{r^2} \mathbf{n} \\ & + \frac{G_{\text{eff}} M}{r^2} \left[\left(\frac{\mathcal{A}_{PN}}{c^2} + \frac{\mathcal{A}_{2PN}}{c^4} \right) \mathbf{n} + \left(\frac{\mathcal{B}_{PN}}{c^2} + \frac{\mathcal{B}_{2PN}}{c^4} \right) \dot{r} \mathbf{v} \right] \\ & + \frac{8}{5} \eta \frac{(G_{\text{eff}} M)^2}{r^3} \left[\left(\frac{\mathcal{A}_{1.5PN}}{c^3} + \frac{\mathcal{A}_{2.5PN}}{c^5} \right) \dot{r} \mathbf{n} \right. \\ & \left. - \left(\frac{\mathcal{B}_{1.5PN}}{c^3} + \frac{\mathcal{B}_{2.5PN}}{c^5} \right) \mathbf{v} \right] \end{aligned} \quad (8)$$

where $\mathbf{x} = \mathbf{x}_1 - \mathbf{x}_2$ is the binary separation, $r = |\mathbf{x}|$, $\mathbf{n} = \mathbf{x}/r$, $\mathbf{v} = \mathbf{v}_1 - \mathbf{v}_2$ is the relative velocity, $\dot{r} = dr/dt$, $M = m_1 + m_2$ is the total mass of the system, and $\eta = (m_1 m_2)/M^2$ is the symmetric mass ratio. The “effective” gravitational constant G_{eff} is related to the gravitational constant G_N measured locally (e.g. by a Cavendish-type experiment) by $G_{\text{eff}} \approx G_N(1 + \alpha_1 \alpha_2)$. Explicit expressions for the functions $\{\mathcal{A}_{\mathcal{I}}, \mathcal{B}_{\mathcal{I}}\}$ are given in Ref. [27] and also depend on the sensitivities/scalar charges of the binary components, e.g. the presence of dissipative 1.5PN terms (which are absent in GR) in Eq. (8) is due to the scalar charges, which source the emission of dipolar gravitational radiation with energy flux

$$\dot{E}_{\text{dipole}} \approx \frac{G_N}{3c^3} \left(\frac{G_{\text{eff}} m_1 m_2}{r^2} \right)^2 (\alpha_1 - \alpha_2)^2. \quad (9)$$

2. Spontaneous, induced and dynamical scalarization

From the dependence of the PN equations on the sensitivities/scalar charges, which in turn depend on the nature and compactness of the binary’s components, it is clear that the PN evolution of a compact-object binary depends on the nature of its components. Therefore, the strong equivalence principle, defined as the universality of free fall for strongly-gravitating objects, is violated in ST theories already in the PN inspiral. Recently, however, Ref. [15] highlighted the existence of other violations of the strong equivalence principle in the last stages of the inspiral of binary neutron stars and for a particular class of ST theories. More specifically, Ref. [15] considered theories with $\omega(\phi) = -3/2 - \kappa/(4\beta \log \phi)$ (or equivalently $\phi = \exp(-\beta\varphi^2)$), which are known [12, 13] to give rise to the “spontaneous scalarization” of isolated neutron stars, i.e. allow for scalar charges $\alpha \sim 0.1 - 1$ for sufficiently compact neutron stars and for viable values of the theory’s parameters $\tilde{\beta} = \beta/(4\pi G) \gtrsim -4.5$ and $\varphi_0 \lesssim 10^{-2}$ (φ_0 being the scalar’s value far from the system). Ref. [15] showed that at sufficiently small binary separations, a spontaneously scalarized star (thus bearing a significant scalar charge) can excite a scalar charge in the other star, even if that star had not spontaneously scalarized and thus did not have a scalar charge to start with. This “induced scalarization” was shown to be capable of triggering earlier binary plunges and mergers

relative to GR, an effect potentially observable with advanced GW detectors [29]. Even more strikingly, Ref. [15] showed that significant scalar charges can be produced in the last inspiral stages of binary systems of unscalerized neutron stars, i.e. in binaries whose components have little or no scalar charges at large separations. This “dynamical scalarization” produces a sudden build-up of the scalar charges at small separations, quickly triggering a plunge/merger at frequencies within the reach of advanced GW detectors (c.f. Ref. [29] for the detectability of this effect with GW detectors).

Remarkably, these two strongly non-linear effects can be understood and reproduced in their main qualitative features by a minimal modification of the PN expansion scheme outline above. More precisely, Ref. [17] describes the evolution of a neutron-star binary system by the PN equations of motion (8), but introduces a new way of computing the sensitivities or scalar charges that appear in those equations. Instead of computing those parameters from isolated neutron-star solutions, as done in the “classic” PN scheme, Ref. [17] introduced a formalism that includes the interaction between the two stars in the calculation of the scalar charges, thus accounting for both induced and dynamical scalarization. In practice, this scheme starts from the standard calculation of the scalar charges for the binary components in isolation, and then uses that calculation to define a system of non-linear algebraic equations, which can be solved iteratively at each step of the PN orbital evolution to yield the charges of both stars including non-linear effects. This procedure was validated by comparing with the fully non-linear simulations of Ref. [15].

3. Electromagnetic coupling in ST theories

One purpose of this paper is to extend the formalism of Ref. [17] to include the effect of an electromagnetic field. Let us consider a binary system of magnetized neutron stars surrounded by a plasma in ST theories. Solving the full non-linear problem in the Jordan frame would require solving the curved spacetime Maxwell equations

$$\partial_{[\mu} F_{\nu\gamma]} = 0, \quad (10)$$

$$\nabla_{\nu} F^{\nu\mu} = j^{\mu}, \quad (11)$$

and including the stress-energy tensor of the electromagnetic field in the source of the Einstein equations. (Note that because of the weak equivalence principle, which is reflected in the structure of the matter action written in Eq. (1), the electromagnetic field only couples to the Jordan frame metric and to the plasma’s electric charges, and not directly to the scalar field.) Introducing the Einstein-frame electromagnetic tensor $F_{\mu\nu}^E = F_{\mu\nu}$ and the plasma’s current $j_E^{\mu} = j^{\mu}/\phi^2$, the Einstein-frame Maxwell equations take the same form as in the Jordan

frame, i.e.

$$\partial_{[\mu} F_{\nu\gamma]}^E = 0, \quad (12)$$

$$\nabla_{\nu}^E F_E^{\nu\mu} = j_E^{\mu}, \quad (13)$$

and the Einstein-frame field equations (3)–(5) become

$$G_{\mu\nu}^E = \kappa (T_{\mu\nu}^{\varphi} + T_{\mu\nu}^{\text{em},E} + T_{\mu\nu}^{\text{pl},E} + T_{\mu\nu}^E), \quad (14)$$

$$\square^E \varphi = \frac{1}{2} \frac{d \log \phi}{d\varphi} (T_E + T_E^{\text{pl}}), \quad (15)$$

$$\nabla_{\mu}^E (T_E^{\mu\nu} + T_{\text{pl},E}^{\mu\nu}) = F_{E\mu}^{\nu} j_E^{\mu} - \frac{1}{2} (T_E + T_E^{\text{pl}}) \frac{d \log \phi}{d\varphi} g_E^{\mu\nu} \partial_{\mu} \varphi, \quad (16)$$

where $T_{\text{em},E}^{\mu\nu} = T_{\text{em}}^{\mu\nu} \phi^{-3}$ is the Einstein-frame stress-energy tensor of the electromagnetic field, while $T_E^{\mu\nu}$ and $T_{\text{pl},E}^{\mu\nu}$ are those of the neutron-star matter and plasma. (Again, all indices are raised and lowered with the Einstein-frame metric.) Note that in deriving these equations we have used

$$\nabla_{\mu}^E T_{\text{em},E}^{\mu\nu} = -F_{E\mu}^{\nu} j_E^{\mu} \quad (17)$$

(which follows from the Maxwell equations), and the fact that the trace of $T_{\text{em},E}^{\mu\nu}$ is zero. Note also that Eq. (15) can be recast in the form

$$\nabla_{\mu}^E T_{\varphi}^{\mu\nu} = \frac{1}{2} \frac{d \log \phi}{d\varphi} (T_E^{\text{pl}} + T_E) g_E^{\mu\nu} \partial_{\mu} \varphi, \quad (18)$$

which shows that in the Einstein frame (as in the Jordan frame) there is no direct energy or momentum transfer from the scalar field to the electromagnetic field.

Postponing the solution to the full non-linear problem to future work, let us note that for astrophysically realistic systems, the plasma and electromagnetic field in the magnetosphere are too small to significantly backreact on the metric and on the binary and scalar field evolution, i.e. to lowest order Eqs. (14)–(16) reduce to Eqs. (3)–(5). To next order, by combining Eqs. (16) and (5) one then obtains

$$\nabla_{\mu}^E T_{\text{pl},E}^{\mu\nu} = F_{E\mu}^{\nu} j_E^{\mu} - \frac{1}{2} T_E^{\text{pl}} \frac{d \log \phi}{d\varphi} g_E^{\mu\nu} \partial_{\mu} \varphi \approx F_{E\mu}^{\nu} j_E^{\mu} \quad (19)$$

where we have used the fact that $T_E^{\text{pl}} \approx 0$ for the plasma (because the particles of which it is made typically move at speeds close to the speed of light) and in any case $d \log \phi / d\varphi \approx 0$ outside the neutron stars (where the plasma moves) because φ is small there. Equation (19) regulates the motion of the plasma, while the electromagnetic field satisfies the Maxwell equations (12)–(13). In both Eq. (19) and Eqs. (12)–(13), the metric is determined by the evolution of the binary and scalar field alone [i.e. by Eqs. (3)–(5)]. In practice, as can be seen from Eq. (7), the scalar field stress-energy vanishes at linear order in the field’s perturbation over a constant background, and is thus negligible outside the neutron stars (although it is not always negligible inside the

stars, where it can grow non-linear and give rise to scalar charges $\alpha \sim 0.1 - 1$ in scalarized systems). Therefore, it is natural to approximate the metric outside the neutron stars with the *general-relativistic* PN metric of two point particles (representing the neutron stars), whose trajectories are calculated (*including* the effect of the scalar charges) with the formalism of Ref. [17]. Therefore, because of Eqs. (12), (13) and (19), the calculation of the electromagnetic fluxes can proceed as in GR, except for the modified binary trajectory. We will present a standard GR approximate strategy to calculate such fluxes (the “unipolar inductor” model) in the next section.

B. Magnetosphere and plasma treatment

As discussed in Ref. [47], neutron stars are surrounded by a magnetosphere with a plasma density $\rho^{pl} \simeq -\vec{\Omega} \cdot \vec{B}/(2\pi c)$, where $\vec{\Omega}$ represents the rotational frequency of the plasma, \vec{B} is the magnetic field present in the region, and c is the speed of light. The interaction of a rotating magnetized star with its own magnetosphere is responsible for electromagnetic emissions in pulsars. The analysis of such interaction is a delicate subject, because the plasma dynamics may be intricate, and complex simulations are typically required to fully capture its behavior. Fortunately, a useful approximation can be adopted that captures important aspects of the system. This approximation relies on the observation that in the magnetosphere region the inertia of the plasma is negligible with respect to the electromagnetic energy density, i.e. $T_{\mu\nu}^{pl} \ll T_{\mu\nu}^{em}$. Through Eqs. (17) and (19), this in turn implies $F_{E\mu}^\nu j_E^\mu \approx F_{\mu j}^\nu \approx 0 \approx \nabla_\mu^E T_{em,E}^{\mu\nu} \approx \nabla_\mu T_{em}^{\mu\nu}$, where in the last passage we have exploited the fact that Eq. (17) also holds in the Jordan frame (as it follows directly from the Maxwell equations (10) and (11)).² These are known as the force-free conditions for the plasma [43, 48, 49], and the resulting electrodynamics equations, while simpler to deal with as now one only needs to consider the behavior of electromagnetic fields constrained by the force-free condition, still represents a non-linear coupled system of partial differential equations. The electrodynamics equations are then augmented by those describing the dynamical behavior of the spacetime and the neutron-star matter, thus complex and time-consuming simulations are typically needed to study the system’s evolution. Nevertheless, for the scenario of interest here – i.e. the late stages of a magnetized binary merger – and for the purpose of our work, we can make use of a hybrid approach, combining the formalism of Ref. [17] described above (whereby the neutron stars are treated as point-like objects satisfying ordinary differential equations of motion

that incorporate the relevant gravitational and scalarization effects) together with a *unipolar model* to account for magnetospheric effects. Both these approaches are supported by simulations of the complete problem in the context of neutron star mergers (for ST theories and non-magnetized systems [17]) and binary neutron star and black hole-neutron star mergers in the context of magnetosphere interactions in GR [36, 37, 42, 50]. As argued in the previous section, a reliable model accounting for magnetosphere interactions within GR should be also applicable to the case of ST theories of gravity. In what follows, we therefore describe the main aspects of the unipolar model.

Magnetosphere interactions and luminosity

A useful model to estimate the electromagnetic energy radiated by a magnetized neutron star binary is based on the *unipolar inductor* [43, 44]. Such a model has recently been further analyzed in Ref. [45] and confronted with fully dynamical simulations including plasma effects, finding good agreement in the obtained luminosity [36, 37, 42]. Similar preliminary conclusions have been obtained in the model’s application to black hole-neutron star binaries [50, 51]. We next describe briefly the main ingredients required by this model for our purposes.

We assume that both stars are magnetized and their magnetic fields are dipolar. Further, we assume that one star has a larger magnetization than its companion, and study the electromagnetic radiation due to the interaction of their magnetospheres. As the orbit tightens, as described in section IIA, ST effects will cause deviations from the GR orbital behavior, which induce a stronger Poynting flux. It is important to stress here that for realistic magnetic fields strengths, electromagnetic effects do not backreact on the orbital evolution of the binary [52, 53]. Under such assumptions, one can estimate the luminosity of the binary [45] as:

$$\mathcal{L} \approx 10^{38} \left(\frac{v_{rel}}{c}\right)^2 \left(\frac{B_*}{10^{11}\text{G}}\right)^2 \left(\frac{R_*}{10\text{km}}\right)^6 \times \left(\frac{R_{eff}}{10\text{km}}\right)^2 \left(\frac{a}{100\text{km}}\right)^{-6} \text{ erg/s} \quad (20)$$

where v_{rel} is the relative velocity of the binary, B_* and R_* are the magnetic field and radius of the primary star and a is the separation between the stars. Induction takes place on the secondary star at a radius R_{eff} , which is equal to the star’s radius R_c when the secondary is unmagnetized. Otherwise, R_{eff} is larger, as the secondary fields shields a region around it. We account for this effect by defining (see Refs. [36, 37, 54]),

$$R_{eff} = \max \left(a \left(\frac{B_c}{B_*}\right)^{1/3}, R_c \right) \quad (21)$$

² One can also show directly that $\nabla_\mu^E T_{em,E\nu}^\mu = \nabla_\mu T_{em,\nu}^\mu / \phi^2$, using the conformal transformation between the Einstein and Jordan frames.

Naturally, this effect is relevant at large separations, while for separations $a \leq R_c \left(\frac{B_c}{B_*}\right)^{-1/3}$ the effective radius reduces to the star's radius R_c . Within GR calculations of the quasi-adiabatic regime of binary neutron star systems (i.e. at large separations), estimates have been obtained from Eq. (20) by replacing v_{rel} with its Keplerian expression and $R_{\text{eff}} = R_c$, giving rise to a dependence $\mathcal{L} \simeq a^{-7}$ (e.g. Refs. [44, 45]). When the shielding effect given by Eq. (21) is considered, the luminosity follows a softer dependence $\mathcal{L} \simeq a^{-5}$ [36, 42]. However, in ST theories, deviations from Keplerian motion are possible, and we thus employ both Eqs. (20) and (21) in our calculations.

III. RESULTS

A. Quasi-circular case

We first study binary systems in quasi-circular (i.e. zero eccentricity) orbits and consider four different sets of masses. These configurations are chosen so that they undergo at least one of the key scalarization processes described in section II A, of course bearing in mind observational constraints for all the physical parameters adopted. More specifically, the configurations we consider are:

- case **LE**, with low- and equal-mass stars ($M_1 = M_2 = 1.41M_\odot$), which undergo dynamical scalarization but do not produce dipolar radiation.
- case **HE**, with high- and equal-masses stars ($M_1 = M_2 = 1.74M_\odot$), which undergo spontaneous scalarization for $\tilde{\beta} = -4.5$ and dynamical scalarization for $\tilde{\beta} = -4.2$, but do not produce dipolar radiation.
- case **LU**, with low- and unequal-mass stars ($M_1 = 1.41M_\odot$, $M_2 = 1.64M_\odot$), which undergo dynamical as well as induced scalarization, and produce dipolar radiation.
- case **HU**, with high- and unequal-mass stars ($M_1 = 1.52M_\odot$, $M_2 = 1.74M_\odot$), which undergo dynamical and induced scalarization (in the lower-mass star) and spontaneous scalarization (in the higher-mass star), and produce dipolar radiation.

Additionally, we consider different possible magnetizations of each star, and examine the characteristics of the resulting electromagnetic luminosity. To adopt realistic configurations, we recall that the standard formation channel of neutron-star binaries indicates that the most likely configurations involve a magnetically dominant (primary) star with a significantly less magnetized companion (secondary) [55–57]. To explore a range of possible options, we consider three ratios of the magnetizations between the stars, namely $b \equiv B_c/B_* = (0.1, 0.01, 0.001)$. Also, for simplicity we assume that the

stars' magnetic dipoles are aligned with the orbital angular momentum. Notice that this is not a restrictive assumption, as it yields reasonably good estimates for the expected power in more general configurations [42]. Finally, we restrict our analysis to the ST theories that yield the largest differences in the binary dynamics, while satisfying existing experimental constraints, i.e. we take the coupling parameter of the ST theory to be $\tilde{\beta} = -4.5$ or $\tilde{\beta} = -4.2$ (so as to satisfy binary pulsar constraints), and we adopt a small value for the asymptotic value of the scalar field $\varphi_0 = 10^{-5}$ to pass solar system tests. For comparison purposes, we also include the corresponding GR results. The list of the cases considered, as well as a summary of the main results (e.g., the total radiated electromagnetic energy for each case), is given in Table I.

As mentioned above, the binary dynamics in ST theories can show clear departures from the GR behavior. In particular, the binary's orbital frequency can increase faster than in GR for high neutron-star masses and low values of $\tilde{\beta}$, because of the enhanced gravitational attraction due to scalar effects and the possible dipolar emission of scalar waves. Such behavior is illustrated in Fig. 1, which shows the separation for the four binaries considered, in ST theories with $\tilde{\beta} = -4.5$ and $\tilde{\beta} = -4.2$, as well as in GR. The complementary Fig. 2 shows how all binary evolutions cover approximately the same frequency range, although for higher masses and lower values of $\tilde{\beta}$, any given frequency is achieved at a larger separation. As discussed, these effects are caused by the scalar charges (or equivalently the sensitivities) that each star acquires as the orbits tighten. The behavior of the scalar charge with respect to separation and orbital frequency for each case considered is shown in Fig. 3, where the orbital frequency is determined instantaneously (i.e. as the derivative of the azimuthal coordinate). From this figure, it is clear that scalarization effects are quite weak in the **LE** case, because the scalar charges remain negligible for most of the evolution and only rise to $\alpha \sim \mathcal{O}(1)$ at relatively short separations (i.e. high frequencies). In particular, the scalar charges remain $\lesssim 10^{-3}$ essentially until the final plunge toward merger. This behavior is in contrast with the remaining cases, where scalarization effects are considerably stronger at the earlier stages, and therefore have a clear impact on the dynamics, especially for $\tilde{\beta} = -4.5$. Such behavior comes about because in the **HE**, **LU** and **HU** cases the more massive star either spontaneously scalarizes already in isolation, which induces a time-dependent running of the scalar charge of the companion (induced scalarization), or both stars scalarize dynamically in the late inspiral (after which the scalar charges further grow by mutual induced scalarization). As mentioned, as the scalar charges grow, the gravitational attraction between the stars gets stronger than in GR, and for unequal-mass binaries the system also emits dipolar radiation, clearly affecting the binary's dynamics.

The dynamical behavior that we have just described has direct consequences on the Poynting flux produced

Case	Masses (in M_\odot)	Magnetic field ratio, $b \equiv B_c/B_*$	Theory	Total E_{rad} [erg]	
				at 35 km	at 30 km
low equal-mass (LE)	$M_1 = 1.41$ $M_2 = 1.41$	0.1	$\tilde{\beta} = (-4.5, -4.2)$; GR	1.74×10^{41}	$(1.90, 1.93, 1.93) \times 10^{41}$
		0.01		4.02×10^{40}	$(4.72, 4.83, 4.83) \times 10^{40}$
		0.001		2.31×10^{40}	$(3.02, 3.12, 3.12) \times 10^{40}$
high equal-mass (HE)	$M_1 = 1.74$ $M_2 = 1.74$	0.1	$\tilde{\beta} = (-4.5, -4.2)$; GR	$(1.27, 1.49, 1.55) \times 10^{41}$	$(1.44, 1.66, 1.78) \times 10^{41}$
		0.01		$(3.06, 3.61, 3.87) \times 10^{40}$	$(4.24, 4.78, 5.42) \times 10^{40}$
		0.001		$(1.74, 2.19, 2.45) \times 10^{40}$	$(2.92, 3.37, 4.01) \times 10^{40}$
low unequal-mass (LU)	$M_1 = 1.41$ $M_2 = 1.64$	0.1	$\tilde{\beta} = (-4.5, -4.2)$; GR	$(1.18, 1.29, 1.41) \times 10^{41}$	$(1.27, 1.49, 1.55) \times 10^{41}$
		0.01		$(2.65, 3.16, 3.24) \times 10^{40}$	$(3.07, 3.61, 3.87) \times 10^{40}$
		0.001		$(1.32, 1.74, 1.83) \times 10^{40}$	$(1.73, 2.19, 2.45) \times 10^{40}$
high unequal-mass (HU)	$M_1 = 1.52$ $M_2 = 1.74$	0.1	$\tilde{\beta} = (-4.5, -4.2)$; GR	$(0.913, 1.05, 1.18) \times 10^{41}$	$(0.996, 1.13, 1.3) \times 10^{41}$
		0.01		$(2.07, 2.37, 2.7) \times 10^{40}$	$(2.45, 2.75, 3.22) \times 10^{40}$
		0.001		$(1.06, 1.2, 1.5) \times 10^{40}$	$(1.43, 1.58, 2.02) \times 10^{40}$

TABLE I: Quasi-circular cases studied in this work. The last two columns show the total electromagnetic energy radiated ($E_{rad} = \int \mathcal{L} dt$) for binaries starting at an initial separation of 180 km apart, until a separation of 35 and 30 km respectively.

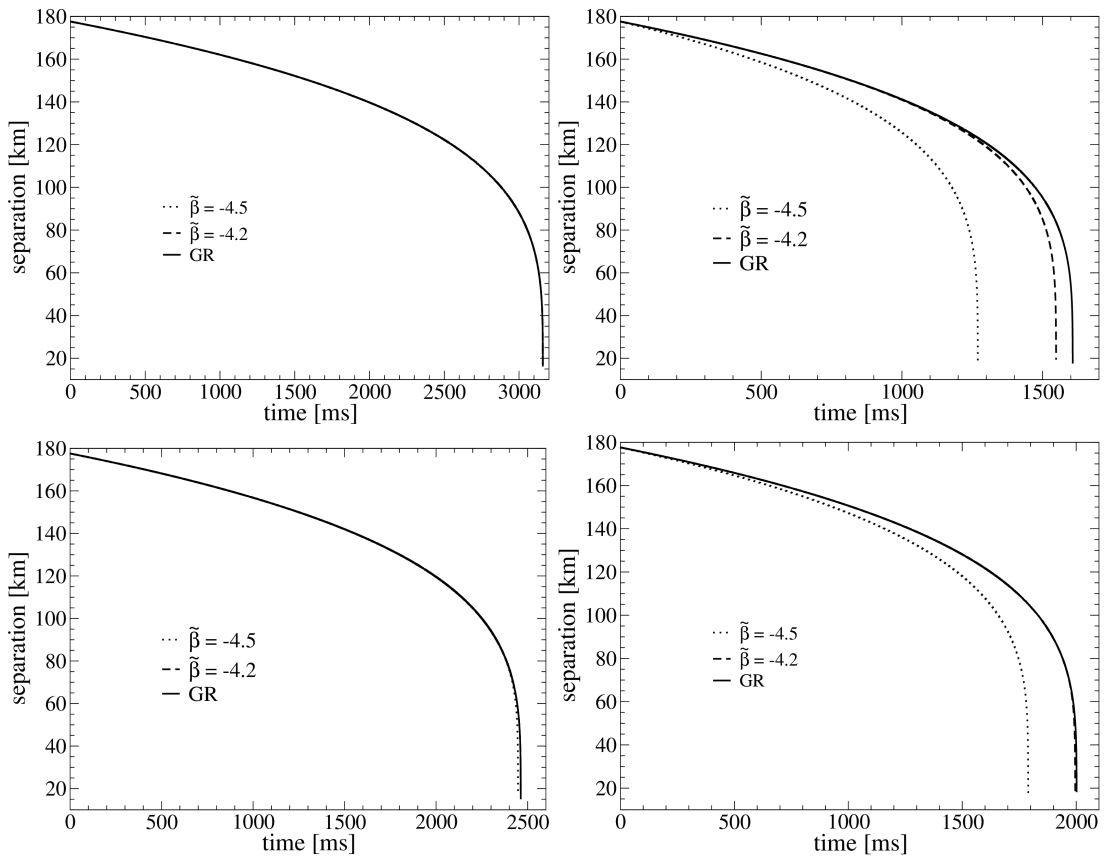


FIG. 1: Separation for the **LE** (top-left panel), **HE** (top-right panel), **LU** (bottom-left panel) and **HU** (bottom-right panel) binaries as a function of time, for $\tilde{\beta} = -4.5$ (dotted lines), -4.2 (dashed lines) and GR (solid lines). Recall that magnetic field effects on the binary's motion are negligible, thus the differences in the trajectories are solely due to the underlying gravity theory. In the **LE** binary, the trajectories for the three cases are almost identical, as there is almost no scalarization until very late in the inspiral. Furthermore, each binary shows different merging times, due to both the different masses involved and the different gravity theories.

by the system as the stars' magnetospheres interact. As described in Sec. II B, we estimate such flux via the enhanced unipolar inductor model, which depends on the orbital evolution as well as on the magnetization of the

binary components. The results for the luminosity are displayed in Figs. 4 and 5 as a function of time and orbital frequency. At a broad level, since all cases cover similar frequency ranges and separations – from ≈ 180

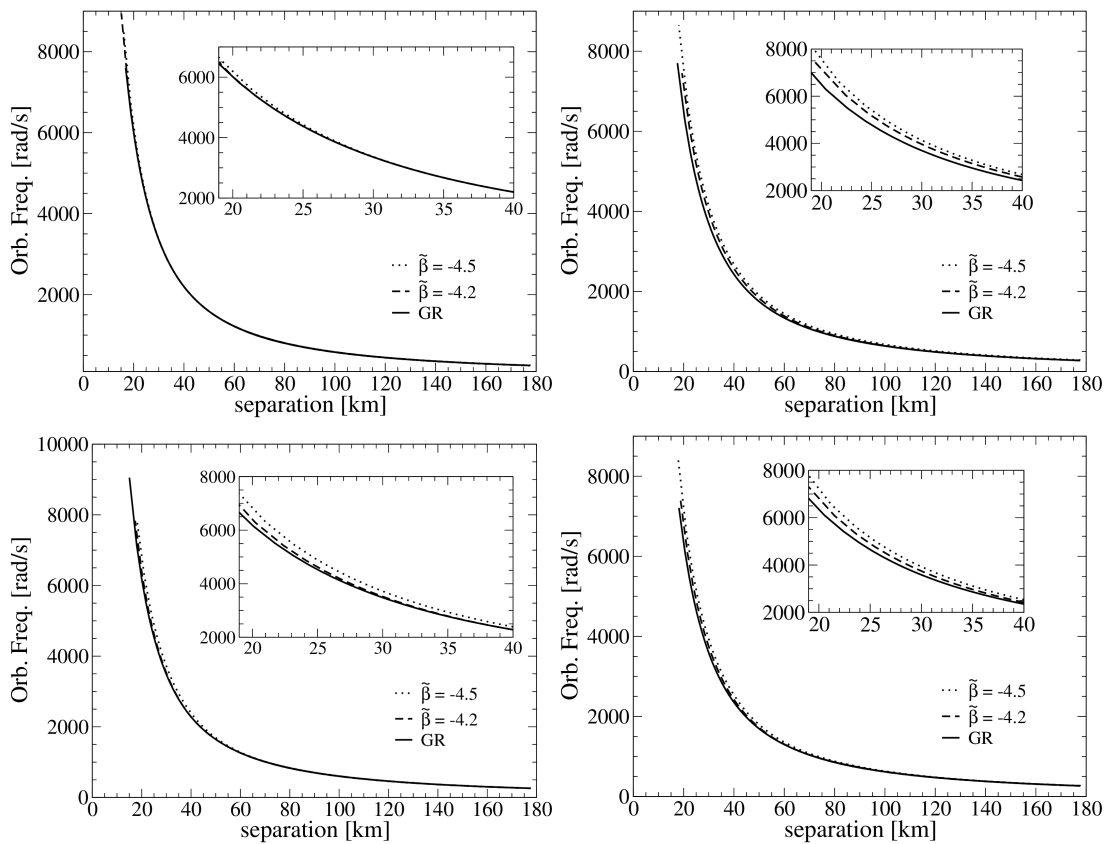


FIG. 2: Orbital frequency as function of separation, for the same parameters shown in Fig. 1.

km to merger for the cases considered – all the obtained luminosities are comparable and on the order of 10^{39} – 10^{41} erg/s (the precise value depending on the binary’s mass and magnetic field ratio between the stars) for a primary with magnetic field of 10^{11} G.

A closer inspection indicates that ST effects are evident at high frequencies for the more massive cases and for lower values of $\tilde{\beta}$. Those systems indeed exhibit a stronger flux, but with a mild dependency on the magnetic-field ratio. Such behavior is more marked in the luminosity rate, as illustrated in Fig. 6. As can be seen, for higher masses and lower values of $\tilde{\beta}$ the dynamics proceeds at a faster pace in ST theories than in GR, thus inducing a more powerful electromagnetic flux. This conclusion is further shown by the total electromagnetic energy radiated as a function of time (Fig. 7), where ST theories of gravity show a clear departure from the general-relativistic behavior.

B. Eccentric binaries

We now turn our attention to binaries with non-negligible eccentricity. Such configurations are not expected to represent a large fraction of the sources detectable by advanced gravitational-wave detectors, as gravitational emission tends to circularize binaries by

the time they enter the detector’s sensitive band. Nevertheless, as already illustrated e.g. in Ref. [58–60], eccentric binaries provide an excellent laboratory to test diverse and extreme physics. As we show here, this is also the case for possible electromagnetic counterparts driven by magnetosphere interactions in non-GR gravity theories. To illustrate this point, we here consider the following two cases: an equal-mass binary with low masses $M_1 = M_2 = 1.52M_\odot$, and an unequal-mass binary with $M_1 = 1.52M_\odot$ and $M_2 = 1.74M_\odot$. Following Ref. [60], we study the dynamics and the emitted electromagnetic flux, in two different configurations: “mild eccentricity” orbits, where the initial apastron/periastron are at separations of about 220 km/80 km respectively (i.e. $e \sim 0.47$); and, “high eccentricity” orbits, where the initial apastron/periastron are at separations of about 220 km/50 km respectively (i.e. $e \sim 0.63$).

These eccentric binaries reveal another interesting phenomenon allowed in ST theories, namely a sequence of successive “scalarization/descalarization” cycles [17]. These produce a strong modulation of the scalar charges (see Fig. 9), with a consequent impact on the dynamics, and possibly observable signatures both in the gravitational and electromagnetic signals. For instance, the binary’s orbit circularizes more rapidly for smaller values of $\tilde{\beta}$ as illustrated in Fig. 9. As can also be seen in that figure, except for the low-, equal-mass binary with

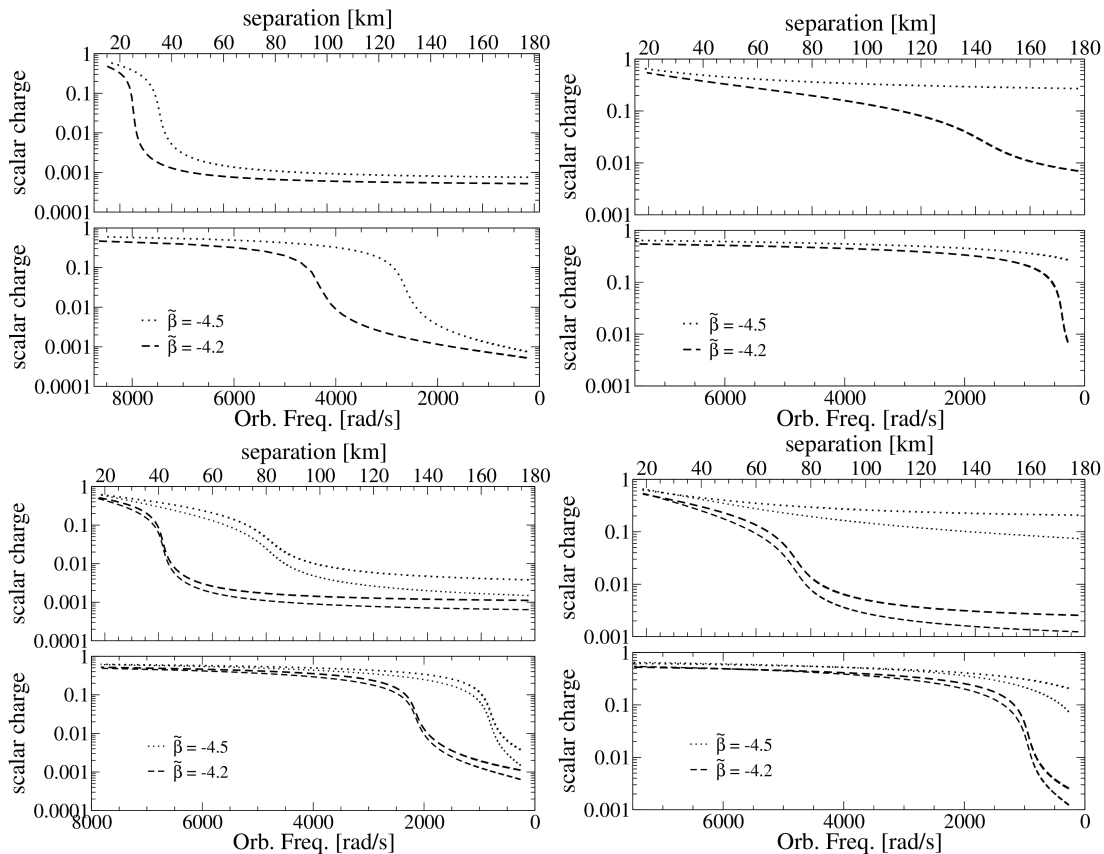


FIG. 3: Scalar charge for the same binaries as in Fig. 1, as a function of the binary separation (first panel) and orbital frequency (second panel), for $\tilde{\beta} = -4.5$ (dotted lines) and -4.2 (dashed lines).

mild eccentricity (which shows negligible differences between GR and ST theories), all the other cases display increasingly marked deviations from GR as $\tilde{\beta}$ decreases and higher masses are considered. This behavior has a direct impact on the electromagnetic flux, as shown in Fig. 10. Of particular interest is the fact that the orbital eccentricity induces, in all cases, an oscillatory behavior in the flux intensity with a frequency and amplitude modulated by a growing trend as the orbit shrinks. Importantly, the growth rate is stronger in the cases governed by ST theories for sufficiently small values of β . Notice additionally that misalignment of the stars' dipole moments induce oscillations in the resulting luminosity even in the quasi-circular case [42].

Finally, we note that the more rapid orbital evolution of strongly scalarized binaries can cause the same total energy to be radiated within a significantly shorter time (see for instance the bottom-right panel of Fig. 11).

IV. DISCUSSION

The results shown in this work indicate that, within the context of electromagnetic emission induced by magnetosphere interactions, binary neutron star systems could

produce signals with clear deviations from the GR expectation, depending on the gravity theory. Our results open up the possibility of exploiting compact binary systems to test gravitational theories by combining electromagnetic and gravitational signals. For instance, in the particular case of ST theories of gravity considered here, deviations in the gravitational-wave signals away from the GR prediction could be detected for binaries that undergo scalarization sufficiently early in the advanced LIGO band [29]. Such binaries, as illustrated here, also show distinctive departures in the Poynting flux luminosity emitted from the system, when compared to the behavior within GR. The fact that deviations could be observed with advanced LIGO if they take place at sufficiently low frequencies in the gravitational-wave signal is a consequence of the detector's sensitivity curve (i.e. sufficiently early scalarization is needed to build up enough signal-to-noise ratio in band). For this reason, scalarization effects at high frequencies in ST theories would be difficult to detect by gravitational-wave signals alone, unless the detector is tuned for higher sensitivity in the higher frequency band. Without such tuning, however, complementary electromagnetic signals could be exploited. As we illustrated here, such opportunity does indeed appear possible.

In particular, our results indicate that a stronger elec-

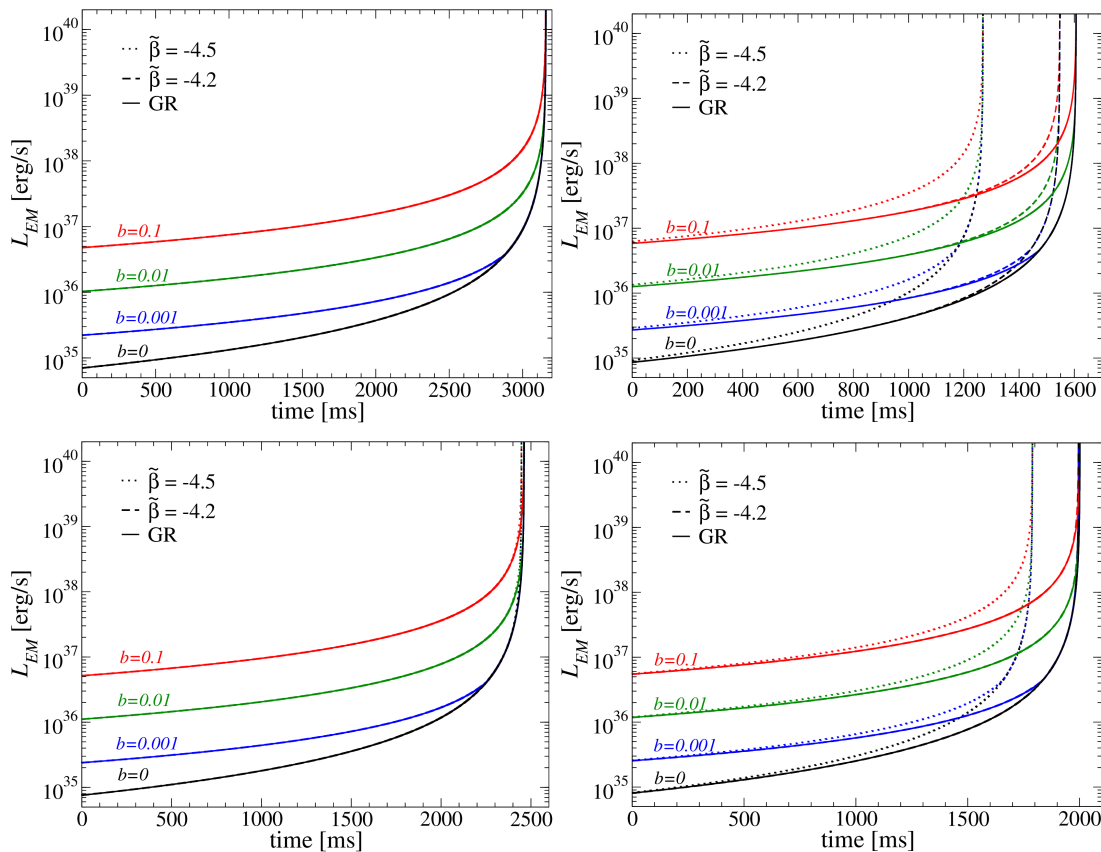


FIG. 4: Luminosity as a function of time, for the same parameters shown in Fig. 1. Different lines in each panel indicate the *ratio* between the secondary and primary magnetic fields (from top to bottom): $b = 0.1$ (in red), $b = 0.01$ (in green), $b = 0.001$ (in blue) and a non-magnetized secondary (i.e. $b = 0$, in black).

tromagnetic luminosity is produced in ST theories for smaller negative values of the coupling $\tilde{\beta}$. This observation is not enough (in itself) to assess the nature of the underlying gravitational theory, unless a good estimate of the stars' magnetization is available. However, we also find that the luminosity's strength and rate of change increase with time is higher in ST theories, and could thus provide precious information that can be used to test the gravity theory. As discussed in Ref. [36], the Poynting flux from binary systems can indeed induce high energy signals from the system which can be exploited for this goal.

Acknowledgments: We thank N. Cornish, L. Samp-

son and N. Yunes for interesting discussions. EB acknowledges support from the European Union's Seventh Framework Programme (FP7/PEOPLE-2011-CIG) through the Marie Curie Career Integration Grant GALFORMBHS PCIG11-GA-2012-321608. LL acknowledges support by NSERC through a Discovery Grant and CIFAR. LL thanks the Institut d'Astrophysique de Paris and the ILP LABEX (ANR-10-LABX-63), for hospitality during a visit supported through the Investissements d'Avenir program under reference ANR-11-IDEX-0004-02. Research at Perimeter Institute is supported through Industry Canada and by the Province of Ontario through the Ministry of Research and Innovation.

-
- [1] E. Adelberger, "Submillimeter tests of the gravitational inverse square law," 2002.
 [2] C. M. Will, "The Confrontation between general relativity and experiment," *Living Rev.Rel.*, vol. 9, p. 3, 2006.
 [3] R. A. Hulse and J. H. Taylor, "Discovery of a pulsar in a binary system," *Astrophys. J. Lett.*, vol. 195, pp. L51–L53, Jan. 1975.
 [4] B. M. Barker and R. F. O'Connell, "Relativistic effects

- in the binary pulsar PSR 1913+16," *Astrophys. J. Lett.*, vol. 199, p. L25, July 1975.
 [5] T. Damour and G. Esposito-Farese, "Gravitational wave versus binary - pulsar tests of strong field gravity," *Phys.Rev.*, vol. D58, p. 042001, 1998.
 [6] J. Antoniadis, P. C. Freire, N. Wex, T. M. Tauris, R. S. Lynch, *et al.*, "A Massive Pulsar in a Compact Relativistic Binary," *Science*, vol. 340, p. 6131, 2013.

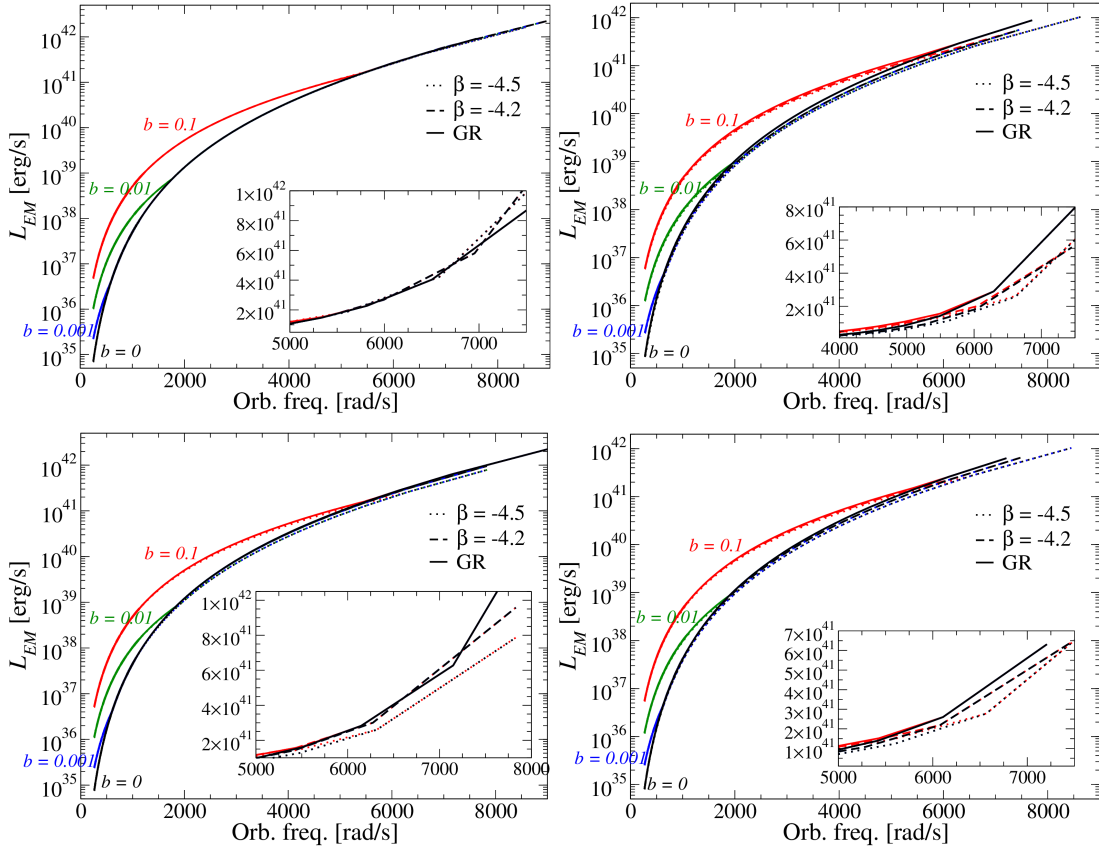


FIG. 5: Luminosity as function of orbital frequency, for the same parameters shown in Fig. 4.

- [7] P. C. Freire, N. Wex, G. Esposito-Farese, J. P. Verbiest, M. Bailes, *et al.*, “The relativistic pulsar-white dwarf binary PSR J1738+0333 II. The most stringent test of scalar-tensor gravity,” *Mon.Not.Roy.Astron.Soc.*, vol. 423, p. 3328, 2012.
- [8] C. M. Will, “Was Einstein right?,” *Annalen Phys.*, vol. 15, pp. 19–33, 2005.
- [9] C. M. Will, *Was Einstein right? Putting general relativity to the test.* 1995.
- [10] D. M. Eardley, “Observable effects of a scalar gravitational field in a binary pulsar,” *Astroph.J.Lett.*, vol. 196, pp. L59–L62, mar 1975.
- [11] C. M. Will and H. W. Zaglauer, “Gravitational Radiation, Close Binary Systems, and the Brans-dicke Theory of Gravity,” *Astrophys.J.*, vol. 346, p. 366, 1989.
- [12] T. Damour and G. Esposito-Farese, “Tensor multi-scalar theories of gravitation,” *Class.Quant.Grav.*, vol. 9, pp. 2093–2176, 1992.
- [13] T. Damour and G. Esposito-Farese, “Nonperturbative strong field effects in tensor - scalar theories of gravitation,” *Phys.Rev.Lett.*, vol. 70, pp. 2220–2223, 1993.
- [14] T. Damour and G. Esposito-Farese, “Tensor - scalar gravity and binary pulsar experiments,” *Phys.Rev.*, vol. D54, pp. 1474–1491, 1996.
- [15] E. Barausse, C. Palenzuela, M. Ponce, and L. Lehner, “Neutron-star mergers in scalar-tensor theories of gravity,” *Phys.Rev.*, vol. D87, p. 081506, 2013.
- [16] M. Shibata, K. Taniguchi, H. Okawa, and A. Buonanno, “Coalescence of binary neutron stars in a scalar-tensor theory of gravity,” 2013.
- [17] C. Palenzuela, E. Barausse, M. Ponce, and L. Lehner, “Dynamical scalarization of neutron stars in scalar-tensor gravity theories,” *Phys.Rev.*, vol. D89, p. 044024, 2014.
- [18] J. S. Bloom, D. E. Holz, S. A. Hughes, K. Menou, A. Adams, S. F. Anderson, A. Becker, G. C. Bower, N. Brandt, B. Cobb, K. Cook, A. Corsi, S. Covino, D. Fox, A. Fruchter, C. Fryer, J. Grindlay, D. Hartmann, Z. Haiman, B. Kocsis, L. Jones, A. Loeb, S. Marka, B. Metzger, E. Nakar, S. Nissanke, D. A. Perley, T. Piran, D. Poznanski, T. Prince, J. Schnittman, A. Soderberg, M. Strauss, P. S. Shawhan, D. H. Shoemaker, J. Sievers, C. Stubbs, G. Tagliaferri, P. Ubertini, and P. Woźniak, “Astro2010 Decadal Survey Whitepaper: Coordinated Science in the Gravitational and Electromagnetic Skies,” *ArXiv e-prints*, Feb. 2009.
- [19] L. Z. Kelley, I. Mandel, and E. Ramirez-Ruiz, “Electromagnetic transients as triggers in searches for gravitational waves from compact binary mergers,” *Phys. Rev. D*, vol. 87, p. 123004, June 2013.
- [20] N. Andersson, J. Baker, K. Belczynski, S. Bernuzzi, E. Berti, *et al.*, “The Transient Gravitational-Wave Sky,” *Class.Quant.Grav.*, vol. 30, p. 193002, 2013.
- [21] L. Lehner and F. Pretorius, “Numerical Relativity and Astrophysics,” 2014.
- [22] L. Sampson, N. Cornish, and N. Yunes, “Mis-Modelling in Gravitational Wave Astronomy: The Trouble With Templates,” *Phys.Rev.*, vol. D89, p. 064037, 2014.
- [23] N. Yunes and F. Pretorius, “Fundamental Theoretic-

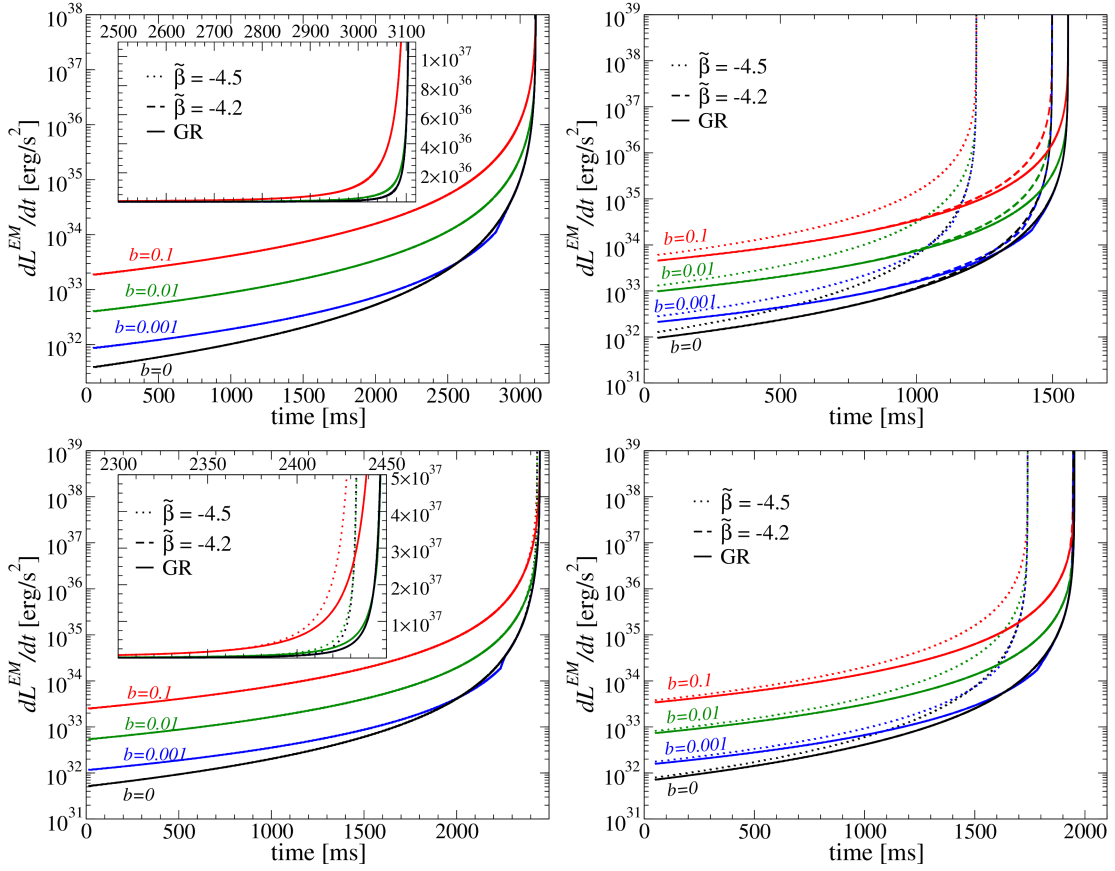


FIG. 6: Time derivative of the luminosity as a function of time, for the same parameters shown in Fig. 4.

- cal Bias in Gravitational Wave Astrophysics and the Parameterized Post-Einsteinian Framework,” *Phys.Rev.*, vol. D80, p. 122003, 2009.
- [24] T. Li, W. Del Pozzo, S. Vitale, C. Van Den Broeck, M. Agathos, *et al.*, “Towards a generic test of the strong field dynamics of general relativity using compact binary coalescence,” *Phys.Rev.*, vol. D85, p. 082003, 2012.
- [25] N. Loutrel, N. Yunes, and F. Pretorius, “A Parametrized post-Einsteinian Framework for Gravitational Wave Bursts,” 2014.
- [26] J. Healy, T. Bode, R. Haas, E. Pazos, P. Laguna, D. M. Shoemaker, and N. Yunes, “Late inspiral and merger of binary black holes in scalar-tensor theories of gravity,” *Classical and Quantum Gravity*, vol. 29, p. 232002, Dec. 2012.
- [27] S. Mirshekari and C. M. Will, “Compact binary systems in scalar-tensor gravity: Equations of motion to 2.5 post-Newtonian order,” *Phys.Rev.*, vol. D87, no. 8, p. 084070, 2013.
- [28] E. Berti, V. Cardoso, L. Gualtieri, M. Horbatsch, and U. Sperhake, “Numerical simulations of single and binary black holes in scalar-tensor theories: circumventing the no-hair theorem,” *Phys.Rev.*, vol. D87, no. 12, p. 124020, 2013.
- [29] L. Sampson, N. Yunes, N. Cornish, M. Ponce, E. Barausse, *et al.*, “Projected Constraints on Scalarization with Gravitational Waves from Neutron Star Binaries,” 2014.
- [30] M. Fierz, “On the physical interpretation of P.Jordan’s extended theory of gravitation,” *Helv.Phys.Acta*, vol. 29, pp. 128–134, 1956.
- [31] P. Jordan, “The present state of Dirac’s cosmological hypothesis,” *Z.Phys.*, vol. 157, pp. 112–121, 1959.
- [32] C. Brans and R. Dicke, “Mach’s principle and a relativistic theory of gravitation,” *Phys.Rev.*, vol. 124, pp. 925–935, 1961.
- [33] P. G. Bergmann, “Comments on the scalar tensor theory,” *Int.J.Theor.Phys.*, vol. 1, pp. 25–36, 1968.
- [34] R. V. Wagoner, “Scalar tensor theory and gravitational waves,” *Phys.Rev.*, vol. D1, pp. 3209–3216, 1970.
- [35] J. Nordtvedt, Kenneth, “PostNewtonian metric for a general class of scalar tensor gravitational theories and observational consequences,” *Astrophys.J.*, vol. 161, pp. 1059–1067, 1970.
- [36] C. Palenzuela, L. Lehner, S. L. Liebling, M. Ponce, M. Anderson, *et al.*, “Linking electromagnetic and gravitational radiation in coalescing binary neutron stars,” *Phys.Rev.*, vol. D88, p. 043011, 2013.
- [37] C. Palenzuela, L. Lehner, M. Ponce, S. L. Liebling, M. Anderson, *et al.*, “Gravitational and electromagnetic outputs from binary neutron star mergers,” *Phys.Rev.Lett.*, vol. 111, p. 061105, 2013.
- [38] K. Kyutoku, K. Ioka, and M. Shibata, “Ultra-Relativistic Counterparts to Binary Neutron Star Mergers in Every Direction, X-ray-to-Radio Bands and Second-to-Day Timescales,” 2012.

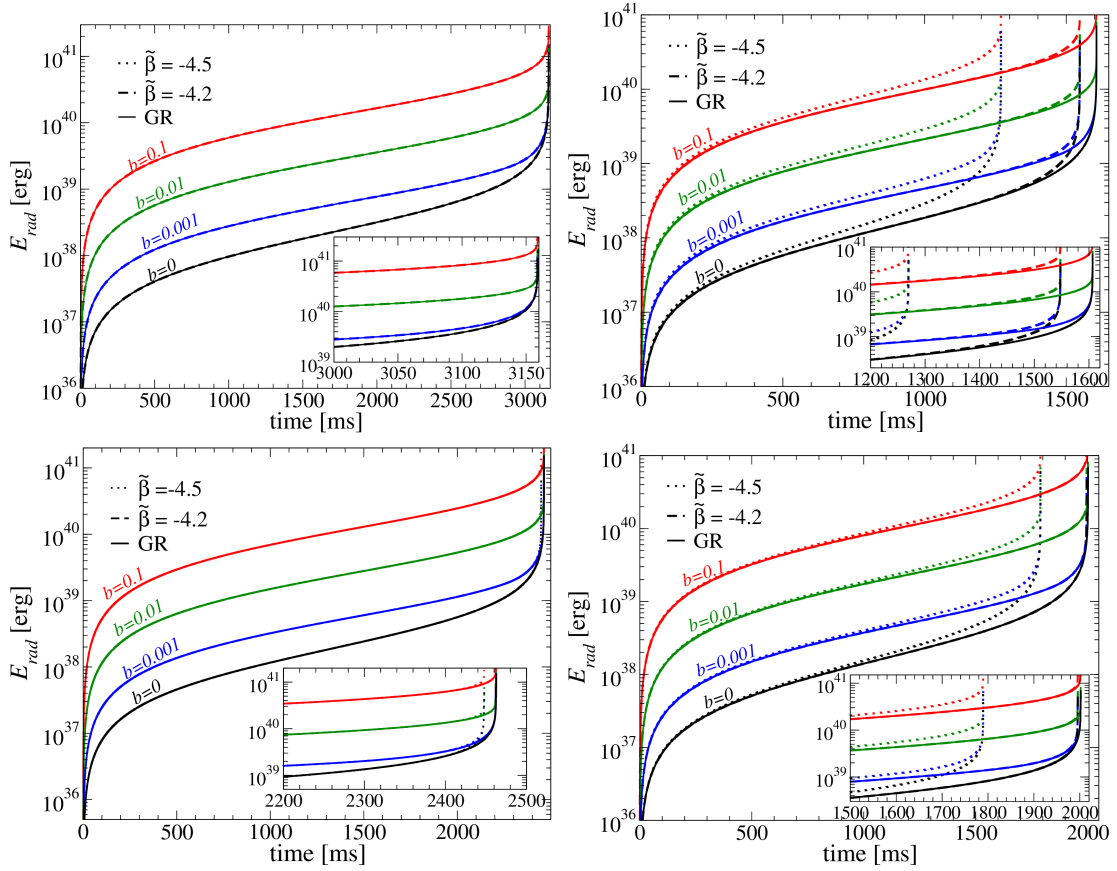


FIG. 7: Total energy radiated in electromagnetic waves (i.e. the time integral of the luminosity) from an initial separation of approx. 180 km, as a function of time, for the same parameters shown in Fig. 4.

- [39] B. D. Metzger and E. Berger, “What is the Most Promising Electromagnetic Counterpart of a Neutron Star Binary Merger?,” *Astrophys. J.*, vol. 746, p. 48, Feb. 2012.
- [40] T. Piran, E. Nakar, and S. Rosswog, “The electromagnetic signals of compact binary mergers,” *Mon. Not. R. Astron. Soc.*, vol. 430, pp. 2121–2136, Apr. 2013.
- [41] D. Tsang *et al.*, “Resonant Shattering of Neutron Star Crusts,” *Phys.Rev.Lett.*, vol. 108, p. 011102, 2012.
- [42] M. Ponce, C. Palenzuela, L. Lehner, and S. L. Liebling, “Interaction of misaligned magnetospheres in the coalescence of binary neutron stars,” *Phys.Rev.*, vol. D90, p. 044007, 2014.
- [43] P. Goldreich and D. Lynden-Bell, “Io, a jovian unipolar inductor,” *Astrophys. J.*, vol. 156, pp. 59–78, Apr. 1969.
- [44] B. M. Hansen and M. Lyutikov, “Radio and x-ray signatures of merging neutron stars,” *Mon.Not.Roy.Astron.Soc.*, vol. 322, p. 695, 2001.
- [45] D. Lai, “DC Circuit Powered by Orbital Motion: Magnetic Interactions in Compact Object Binaries and Exoplanetary Systems,” *Astrop. J. Lett.*, vol. 757, p. L3, 2012.
- [46] J. Healy, T. Bode, R. Haas, E. Pazos, P. Laguna, *et al.*, “Late Inspiral and Merger of Binary Black Holes in Scalar-Tensor Theories of Gravity,” 2011.
- [47] P. Goldreich and W. H. Julian, “Pulsar Electrodynamics,” *Astrophys. J.*, vol. 157, p. 869, Aug. 1969.
- [48] R. D. Blandford and R. L. Znajek, “Electromagnetic extraction of energy from Kerr black holes,” *Mon. Not. R. Astron. Soc.*, vol. 179, pp. 433–456, May 1977.
- [49] S. S. Komissarov, “Time-dependent, force-free, degenerate electrodynamics,” *Mon. Not. R. Astron. Soc.*, vol. 336, pp. 759–766, Nov. 2002.
- [50] V. Paschalidis, Z. B. Etienne, and S. L. Shapiro, “General relativistic simulations of binary black hole-neutron stars: Precursor electromagnetic signals,” *Phys.Rev.*, vol. D88, no. 2, p. 021504, 2013.
- [51] S. T. McWilliams and J. Levin, “Electromagnetic Extraction of Energy from Black-hole-Neutron-star Binaries,” *Astrophys. J.*, vol. 742, p. 90, Dec. 2011.
- [52] K. Ioka and K. Taniguchi, “Gravitational waves from inspiralling compact binaries with magnetic dipole moments,” *Astrophys.J.*, 2000.
- [53] M. Anderson, E. W. Hirschmann, L. Lehner, S. L. Liebling, P. M. Motl, *et al.*, “Magnetized Neutron Star Mergers and Gravitational Wave Signals,” *Phys.Rev.Lett.*, vol. 100, p. 191101, 2008.
- [54] L. Lehner, C. Palenzuela, S. L. Liebling, C. Thompson, and C. Hanna, “Intense electromagnetic outbursts from collapsing hypermassive neutron stars,” *Phys. Rev. D*, vol. 86, p. 104035, Nov. 2012.
- [55] A. Cumming, E. Zweibel, and L. Bildsten, “Magnetic Screening in Accreting Neutron Stars,” *Astrophys.J.*, vol. 557, pp. 958–966, Aug. 2001.
- [56] D. R. Lorimer, “Binary and millisecond pulsars,” *Living*

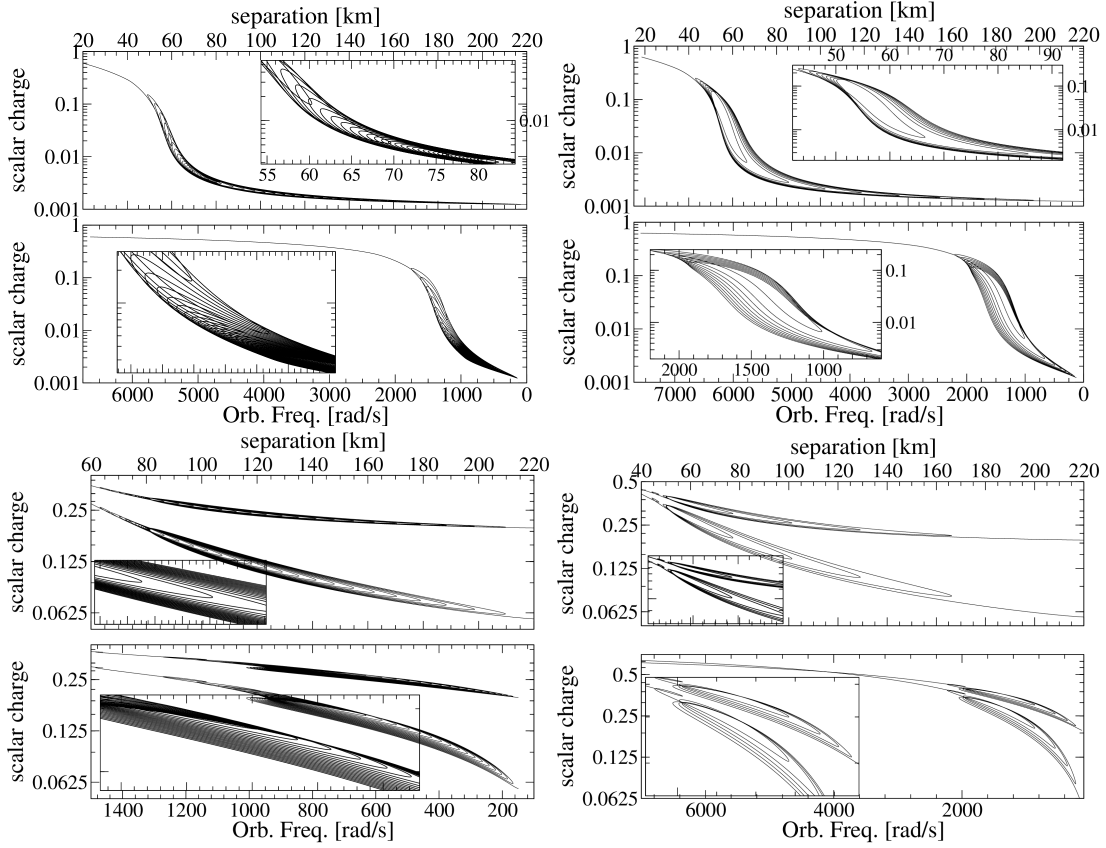


FIG. 8: Eccentric Binaries: evolution of the scalar charges as a function of separation and orbital frequency, for an equal-mass binary (top panels) and an unequal-mass binary (bottom panels), for low-eccentricity orbits (left column) and high-eccentricity orbits (right column); see text for the details on the exact masses and eccentricities. The insets show zoom-in regions displaying a sort of “nested” curves (similar to those showed in Fig. 20 from Ref. [17]). For clarity’s sake we illustrate here one case of the ST theory, $\tilde{\beta} = -4.5$.

Reviews in Relativity, vol. 11, no. 8, 2008.

- [57] K. A. Postnov and L. R. Yungelson, “The evolution of compact binary star systems,” *Living Reviews in Relativity*, vol. 9, no. 6, 2006.
- [58] J. Healy, J. Levin, and D. Shoemaker, “Zoom-Whirl Orbits in Black Hole Binaries,” *Phys.Rev.Lett.*, vol. 103, p. 131101, 2009.

- [59] R. Gold, S. Bernuzzi, M. Thierfelder, B. Bruggmann, and F. Pretorius, “Eccentric binary neutron star mergers,” *Phys.Rev.*, vol. D86, p. 121501, 2012.
- [60] W. E. East and F. Pretorius, “Dynamical Capture Binary Neutron Star Mergers,” *Astrophys.J.*, vol. 760, p. L4, 2012.

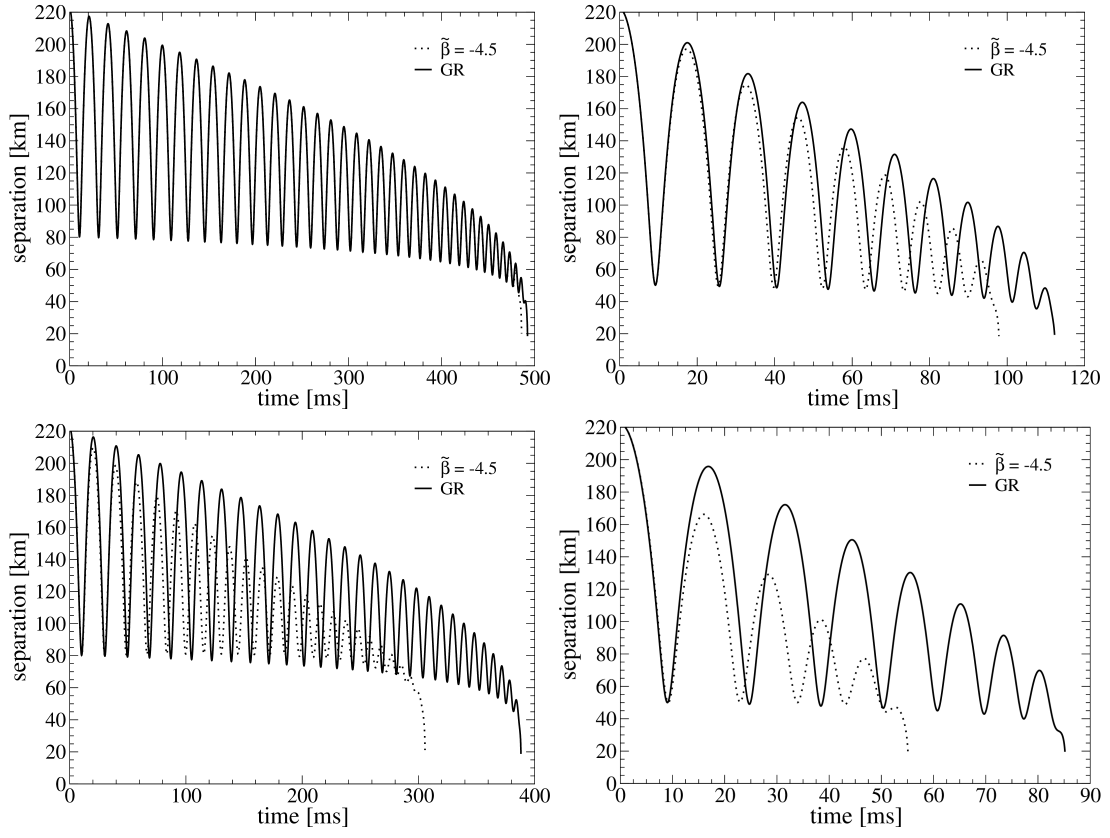


FIG. 9: Eccentric Binaries: evolution of the separation as a function of time, for the same cases as in Fig. 8.

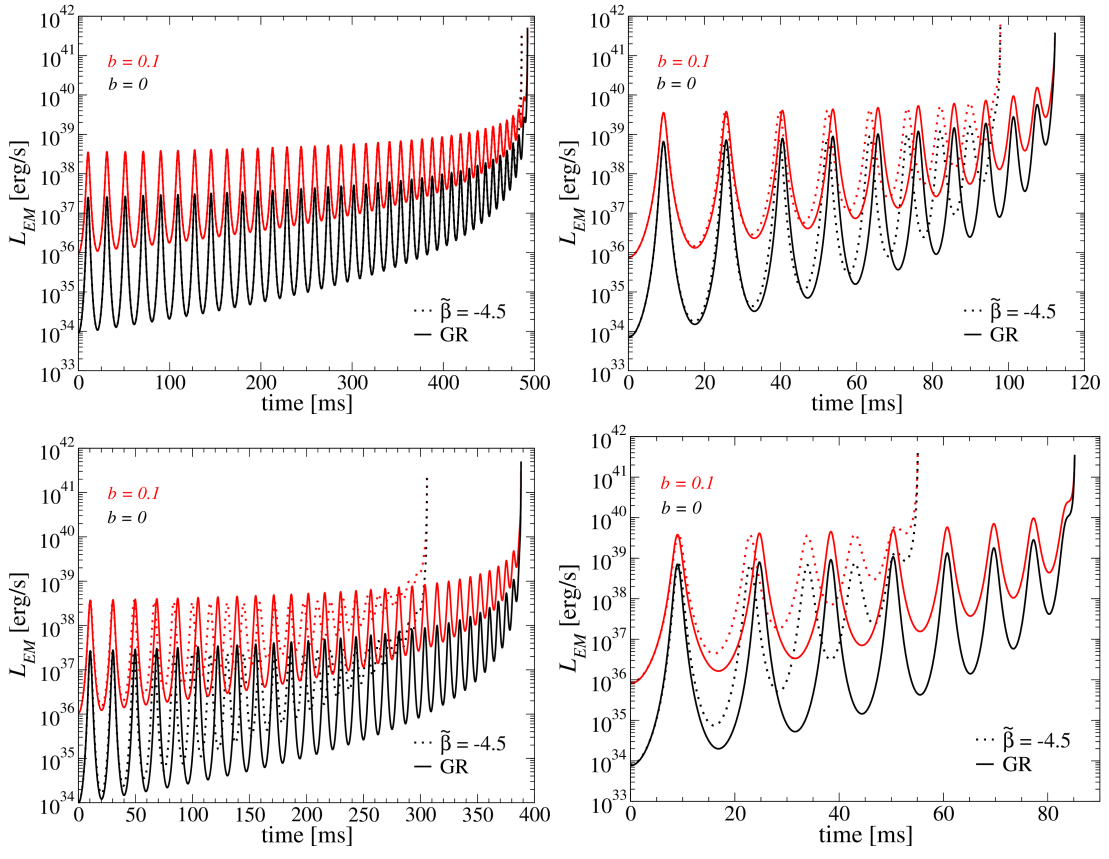


FIG. 10: Luminosity vs time, for the same parameters shown in Fig. 9. For clarity's sake we show here the two extremal magnetic ratios considered, $b = 0.1$ and $b = 0$ (i.e. a non-magnetized companion).

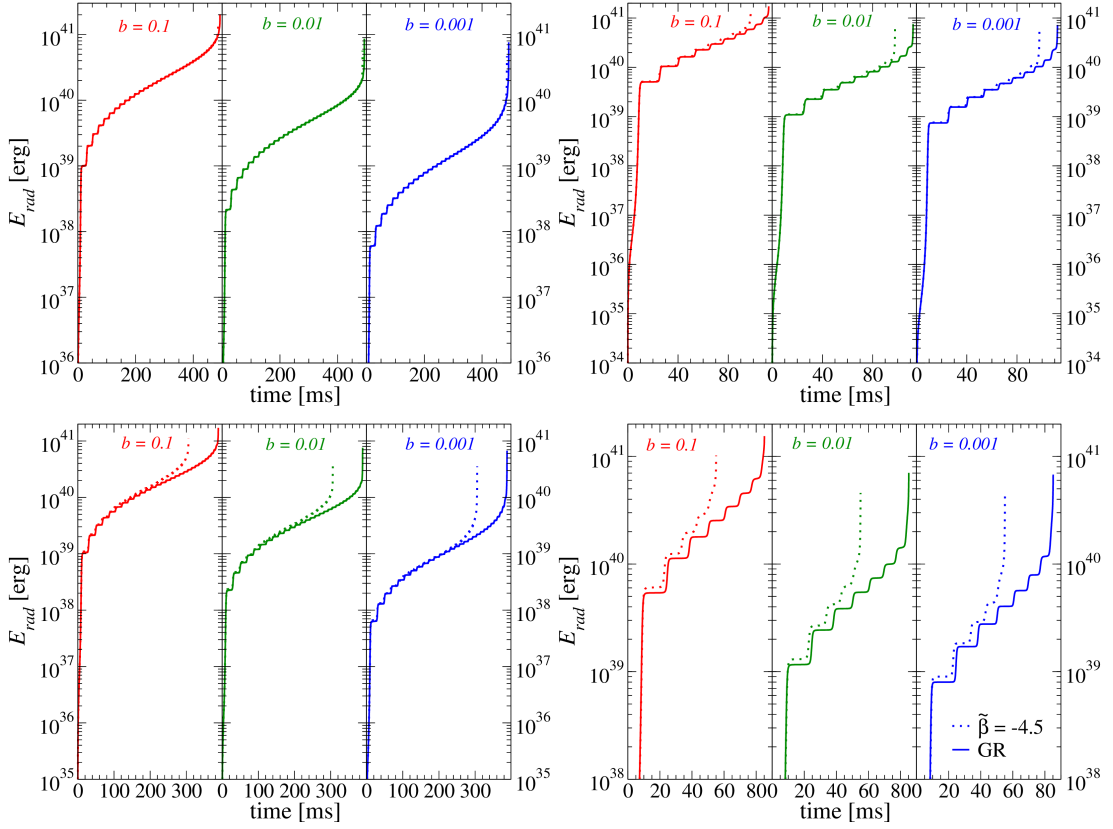


FIG. 11: Radiated energy from the eccentric binaries with an initial separation of approx. 220 km as a function of time, for the same parameters shown in Fig. 9. We show in contiguous panels, three different magnetic ratios (from left to right within each plot): $b = 0.1$ (in red), 0.01 (in green), and 0.001 (in blue). Notice that in the case of low-eccentricity orbits (left column), the radiated energy has a smoother (continuous) trend, while in the case of high-eccentricity orbits (right column) the radiated energy is more jagged; this is a consequence of the oscillatory features in the luminosity, and ultimately the effect of the different dynamics of each binary.